Australian Journal of Basic and Applied Sciences, 5(10): 1374-1378, 2011
ISSN 1991-8178

Analysis of Lattice Temperature Effects on a Long Wavelength InGaAsP Photonic Crystal VCSEL

[1]Saeid Marjani and [2]Hamid Marjani

[1]Young Researchers Club, Arak Branch, Islamic Azad University, Arak, Iran.
[2]Department of Electrical Engineering, Arak Branch, Islamic Azad University, Arak, Iran.

Abstract: Simulative study on the effects of lattice temperature on a Long Wavelength InGaAsP Photonic Crystal vertical-cavity surface-emitting laser (VCSEL) is presented, in this paper. Loss mechanisms are well known from the edge- emitting lasers (EELs), but they are severe in VCSELs. This is due to the optical wavelength cannot follow the thermal shift of the gain peak. As a consequence, the wall-plug efficiency and the differential quantum efficiency are very sensitive to changes in temperature. The device employs InGaAsP active region, which is sandwiched between GaAs/AlGaAs and GaAs/AlAs distributed Bragg reflectors (DBRs). This paper provides key results of the wall-plug efficiency and the differential quantum efficiency upon the lattice temperature.

Key words: Wall-plug efficiency, Differential quantum efficiency, Lattice temperature, Photonic Crystal, VCSEL

INTRODUCTION

Vertical-cavity surface-emitting lasers (VCSELs) offer several favorable characteristics in comparison to conventional edge emitting devices(EELs), such as single-mode operation, low threshold current, high-output power, high speed modulation, a circular beam profile and low manufacture cost. In recent years, long wavelength (1.565 μm - 1.625 μm) PhC VCSELs have been a subject of intensive research efforts due to their important role in high performance optical communication systems, since they permit higher bit rates over longer distances while persevering in the cost factor (Dems *et al*., 2005). High optical gain in the active area and high thermal conductivity in the reflecting mirrors are the main difficulties in developing VCSELs which are used in the field of optical spectroscopy (Kapon and Sirbu, 2009).

Lattice heat is generated whenever physical processes transfer energy to the crystal lattice. According to differences in transfer mechanisms, heat sources can be separated into Joule heat, electron–hole recombination heat, Thomson heat, and heat from optical absorption. Self-heating often limits the performance of optoelectronic devices. Heat is generated when carriers transfer part of their energy to the crystal lattice. In consequence, the thermal energy of the lattice rises, which is measured as an increase in its temperature (Piprek, 2003). The simultaneous demonstration of high temperature, high power lasing is the main challenge in developing VCSELs (Piprek *et al*., 2004).

In this paper, we attempt to evaluate the effect of lattice temperature on the efficiencies of a Long Wavelength InGaAsP PhC VCSEL using numerically-based simulation software (SILVACO, 2010).

In the following, we first briefly describe the numerical model and the details of the PhC VCSEL structure. Next we present the obtained numerical results. Finally, the conclusions provide common guidelines for designing performance of PhC VCSELS.

II. Theory:

In simulation VCSEL, we must consider the electrical, optical and thermal interaction during VCSEL performance. Base of simulation is to solve Poisson and continuity equations for electrons and holes (SILVACO, 2010). Poisson's equation is defined by:

$$\nabla \bullet \left(\in \nabla \Psi \right) = \rho \tag{1}$$

where ψ is electrostatic potential, ρ is local charge density and ε is local permittivity. The continuity equations of electron and hole are given by (Piprek *et al*., 2004):

$$\frac{\partial n}{\partial t} = G_n - R_n + \frac{1}{q} \nabla . \vec{J}_n \tag{2}$$

$$\frac{\partial p}{\partial t} = G_p - R_p + \frac{1}{q} \nabla . \vec{J}_p \tag{3}$$

where n and p are the electron and hole concentration, J_n and J_p are the electron and hole current densities, G_n and G_p are the generation rates for electrons and holes, R_n and R_p are the recombination rates and q is the magnitude of electron charge.

Corresponding Author: Saeid Marjani, Young Researchers Club, Arak Branch, Islamic Azad University, Arak, Iran.
E-mail: saeidmarjani@yahoo.com

The fundamental semiconductor equations (1)-(3) are solved self-consistently together with Helmholtz and the photon rate equations. The applied technique for the solution of Helmholtz equation is based on the improved effective index model (Wenzel and Wunsche, 1997), which shows accuracy for the great portion of preliminary problems. This model is very well adapted to simulation of VCSEL structures, and it is often called effective frequency method (Numai, 2004). Two-dimensional Helmholtz equation is solved to determine the transverse optical field profile, and it is given by (SILVACO, 2010):

$$\frac{dS_m}{dt} = (\frac{c}{N_{eff}} G_m - \frac{1}{\tau_{ph_m}} - \frac{cL}{N_{eff}}) S_m + R_{sp_m} \tag{4}$$

where ω is the frequency, ε(r, z, φ, ω) is the complex dielectric permittivity, E(r, z, φ) is the optical electric field and c is the speed of light in the vacuum.

The light power equation relates electrical and optical models. The photon rate equation is given by (SILVACO, 2010):

$$\nabla^2 E(r,z,\varphi) + \frac{\omega_0}{c^2} \varepsilon(r,z,\varphi,\omega) E(r,z,\varphi) = 0 \tag{5}$$

where S_m is the photon number, G_m is the modal gain, R_{sp_m} is the modal spontaneous emission rate, L represents the losses in the laser, N_{eff} is the group effective refractive index, τ_{ph_m} is the modal photon lifetime and c is the speed of light in the vacuum. The m refers to modal number. The modal gain is (Hadley, 1995):

$$G_m = \iiint g_m(r,z).\left|E_m(r,z)\right|^2 r d\theta dr dz \tag{6}$$

where $E_m(r, z)$ is the normalized optical field.

And modal of spontaneous emission rate is (SILVACO, 2010):

$$R_{sp_m} = \iiint r_{sp}(r,z)_m r d\theta dr dz \tag{7}$$

The modal photon lifetime, τ_{ph_m}, determines losses in laser and it is given by (SILVACO, 2010):

$$\frac{1}{\tau_{ph_m}} = \frac{c}{NEFF}\left(\alpha_{a_m} + \alpha_{fc_m} + \alpha_{mir}\right) = \frac{c}{NEFF} G_m - \omega_0 . \nu_{lm} \tag{8}$$

where α_a is losses of bulk absorption, α_{fc} is losses of free-carriers, α_{mir} is losses of mirrors and υ_{lm} is a parameter of dimensionless frequency.

The heat flow equation has the form (SILVACO, 2010):

$$C\frac{\partial T_L}{\partial t} = \nabla(\kappa \nabla T_L) + H \tag{9}$$

where C is the heat capacitance per unit volume, κ is the thermal conductivity, H is the generation, T_L is the local lattice temperature and H is the heat generation term.

Eq.(1)-(9) provide an approach that can account for the mutual dependence of electrical, thermal, optical and elements of heat sources.

III. VCSEL structure:

Fig.1 shows the schematic structure of PhC VCSEL device. Thirty periods of $GaAs/Al_{0.33}Ga_{0.67}$ with index of refraction of layers 3.38 and 3.05 respectively, form the top and layer interfaces are parabolically graded to reduce interface electrical resistance. The InGaAsP multi quantum well (MQW) consists of six quantum wells where the well is 5.5nm $In_{0.76}Ga_{0.24}As_{0.82}P_{0.18}$ and the barrier is 8nm $In_{0.48}Ga_{0.52}As_{0.82}P_{0.18}$. It is embedded in InP spacer layers that have been extended by thin GaAs layers on top of each fused mirror to increase the emission wavelength. The bottom 28-period GaAs/AlAs DBR with index of refraction of layers 3.38 and 2.89 respectively, is pulse doped at all interfaces. Triangular-lattice air holes are formed in the upper pairs of top DBR. The optical confinement is achieved by means of seven air holes where the center is missed off to make the defect region, as shown in Fig.2.

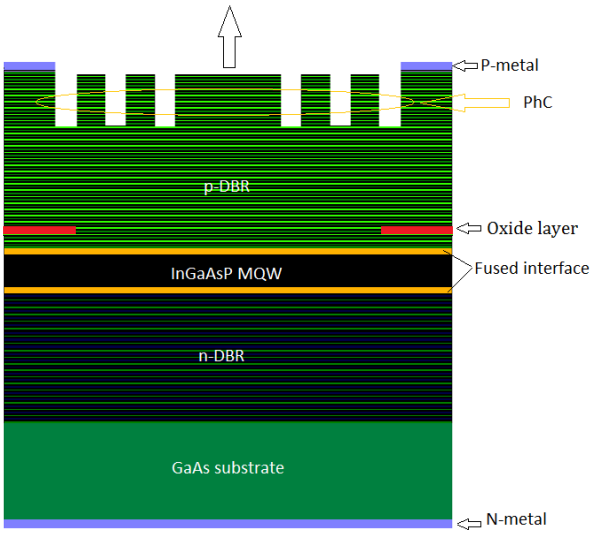

Fig. 1. Schematic structure of the PhC VCSEL device

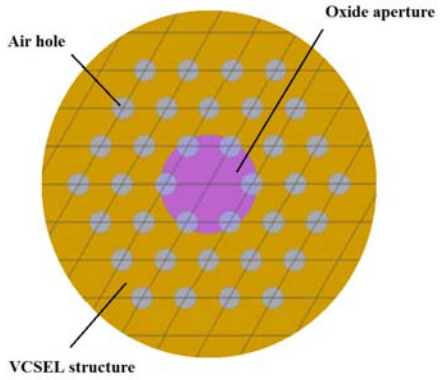

Fig. 2. Top view of the triangular-lattice air holes pattern.

*IV. **Results:***

Heat loss from the modeled PhC VCSEL device was specified using thermal contacts at the top electrode, bottom electrode and the device sidewall. The thermal contacts define thermal conductivities to simulate heat loss from radiation via exposed surfaces or conduction through the semiconducting material to a heatsink.

Fig.3 shows the 2D model of the Phc VCSEL device with a contour plot of the lattice temperature. As can be seen from Fig.3, the thermal resistance used to model the electrical contacts causes about 8 K temperature increment above the ambient temperature (300 k) at a bias of 3 V.

The wall-plug efficiency is of highest importance for many applications, and VCSELs are attractive devices because high wall-plug efficiencies can be obtained with relatively low input powers (Numai, 2004). The wall-plug efficiency equation is given by (Alias *et al*., 2006):

$$\eta_{wp} = \frac{P_{out}}{IV} \tag{10}$$

where Pout is the output optical power, I is the injection current and V is bias voltage. The differential quantum efficiency equation is given by (Alias *et al*., 2006):

$$\eta_D \approx \frac{dP}{dI}\frac{1}{E_g} \tag{11}$$

where E_g is the bandgap energy. The lattice temperature was varied between 280 K until 370 K and its effects on the wall-plug efficiency and the differential quantum efficiency curves are shown in Fig.4, Fig.5, respectively.

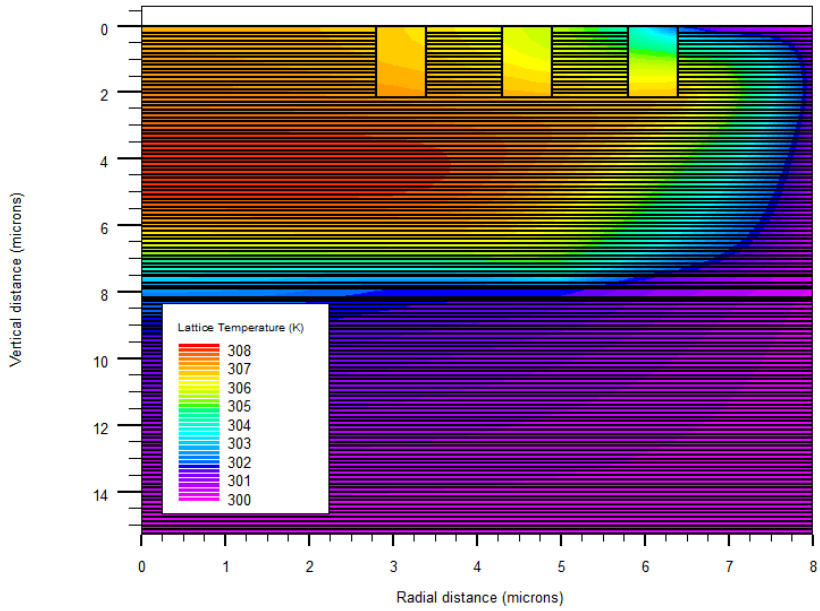

Fig. 3. 2D model of the Phc VCSEL device with a contour plot of the lattice temperature.

As can be seen from Fig.4 and Fig.5, increasing of the lattice temperature causes the reduction of both the wall-plug efficiency and the differential quantum efficiency. This decrement should be mainly due to the combined effects of Auger processes, valence band absorptions and free carrier absorptions. At high temperature, electrons leak out of the QWs into the barriers due to the small conduction band offset. Unbalanced charge distribution between the QWs and the barriers causes an electric field that traps holes in the barriers and increases the internal absorption loss and recombination. Furthermore, Fig.4 and Fig.5 show a decrement in wall-plug efficiency (27.795 % at 1.5 V to 22.318 % at 2.5 V at 300 K) and an increment in the differential quantum efficiency (34.145 % at 1.5 V to 41.29 % at 2.5 V at 300 K) with increment in operating voltage.

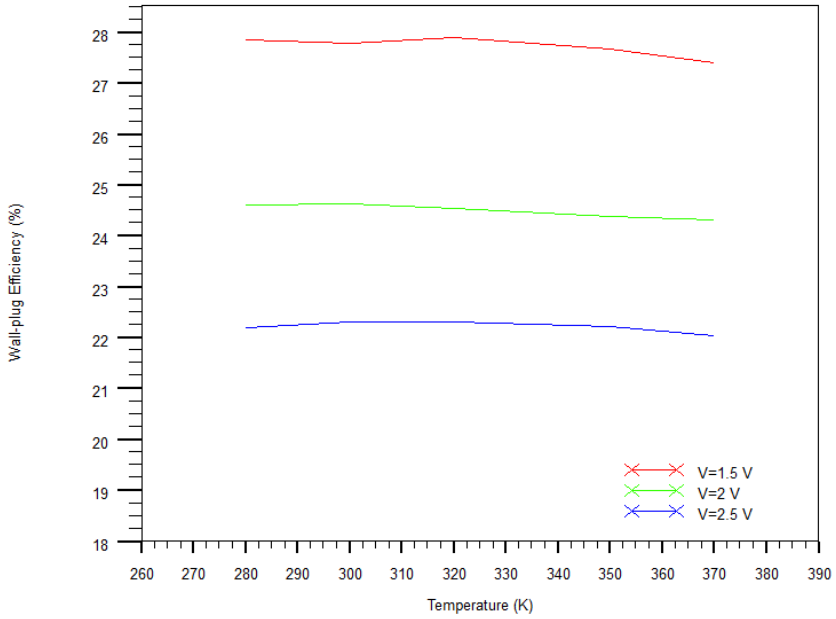

Fig. 4. Wall-plug efficiency versus lattice temperature as a function of bias voltage

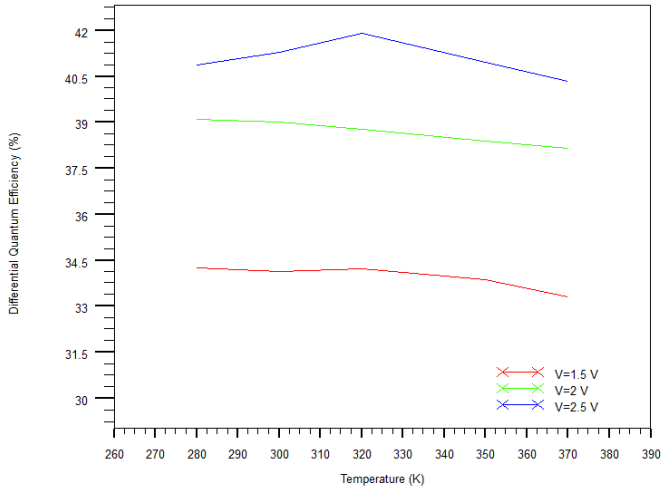

Fig. 5. Differential quantum efficiency versus lattice temperature as a function of bias voltage.

Conclusion:

In this paper, we have shown the lattice temperature have a profound impact on the PhC VCSEL the wall-plug efficiency and the differential quantum efficiency that operating in the 1570 nm wavelength regime. The results indicate that increasing of the lattice temperature causes the reduction of both the wall-plug efficiency and the differential quantum efficiency.

REFERENCES

Alias, M.S., P.O. Leisher, K.D. Choquette, K. Anuar, D. Siriani, S. Mitani, Y.M. Razman, A.M.A. Fatah, 2006. "Electro-Opto Characteristics of 850 nm Oxide-Confined Vertical-Cavity Surface- Emitting Lasers"; IEEE Int. Conf. on Semiconductor Electronics ICSE2006: 227-230.

Dems, M., R. Kotynski and K. Panajotov, 2005. "Plane Wave Admittance Method - a novel approach for determining the electromagnetic modes in photonic structures," J. Opt. Express., 13: 3196-3207.

Hadley, G.R., 1995. "Effective index model for vertical-cavity surface-emitting lasers," J. Opt. Lett., 20: 1483-1485.

Kapon, E., A. Sirbu, 2009. "Power-efficient answer," Nature Photonics., 3: 27-29.

Numai, T., 2004. "Fundamentals of Semiconductor Lasers"; Springer Series in Optical Sciences, New York.

Piprek, J., 2003. Semiconductor Optoelectronic Devices: Introduction to Physics and Simulation Academic Press, San Diego.

Piprek, J., M. Mehta and V. Jayaraman, 2004. "Design and Optimization of high-performance 1.3 um VCSELs," Proc. of SPIE5349.

SILVACO International Incorporated, 2010. ATLAS User's Manual, Version 5.12.0.R. SILVACO, Inc., USA.

Wenzel, H., H.-J. Wunsche, 1997. "The effective frequency method in the analysis of vertical-cavity surface-emitting lasers," J. IEEE Quantum Electronics., 33: 1156.